

Constrained 3D modelling and geochemical analyses of the Horseshoe Range BIF: tools for evaluating magnetic signatures under cover

Ben Patterson *
CSIRO Mineral Resources
North Ryde, NSW
Ben.Patterson@csiro.au

Dr James Austin
CSIRO Mineral Resources
North Ryde, NSW
James.Austin@csiro.au

Dr Mark Pearce
CSIRO Mineral Resources
Kensington, WA
Mark.Pearce@csiro.au

SUMMARY

The Horseshoe Range is a banded iron formation (BIF) in the Southern Capricorn Orogen, WA and is associated with a large horseshoe-shaped positive magnetic anomaly. Electron microscope mineralogy identified ubiquitous goethite and magnetite/hematite. This study focussed on measuring the magnetic properties of the rocks at Horseshoe Range in order to accurately predict their geophysical responses when buried beneath cover.

Remanent magnetisation intensities of the rocks were high (up to 1300 A/m) and vectors measured in the rocks were oriented predominately downward which typically result in negative anomalies which is inconsistent with the observed anomaly. Due to the positive nature of the magnetic anomaly and the ability to accurately model the response without remanent magnetisation it appears that the high intensity remanent magnetisations may be volumetrically insignificant and likely limited to the near surface. The remanence may be caused by near surface formation of maghemite during bushfires and/or induced by lightning strikes.

The BIF can be modelled using a single homogenous layer with a susceptibility of 0.8 SI. However, this is not geologically consistent with BIFs which typically display variable iron-oxide mineralogy and associated petrophysical properties. One way to more accurately model BIFs is to use the first vertical derivative as the model input. Using this approach, a 4 layer model was generated which matched the anomaly to an RMS of ~1%. Modelled susceptibilities ranged from 0.01 – 0.55 SI which are consistent with the measured properties. However, this model did not take into account the measured high intensity downward magnetisation vectors.

Key words: Palaeomagnetism, AMS, BIF, petrophysics, hematite, magnetite

INTRODUCTION

The Horseshoe Range BIF sits within the southern Capricorn Orogen in Western Australia. The main mineral deposits in the region are dominantly iron ore deposits of the Hammersley Basin although a number of high grade polymetallic deposits have also been found in the central and southern parts of the Orogen including Degruusa, Plutonic and Fortnum. Both the polymetallic base-metal deposits and manganese-rich BIF styles of mineralisation have distinct geophysical expressions. Hence, investigation of their petrophysical properties, their structural properties and the influence of mineralogy and structure on such properties may help constrain future exploration, particularly in covered areas of the province. The local geology is comprised predominately of layered iron-oxide rich siltstones interlayered with cherty bands (i.e. BIFs) of the Horseshoe Formation, a member of the Bryah Basin. Bedding generally dips to the southwest and the axis of the Horseshoe Fold itself plunges towards the southwest. Small metre-decimetre scale folds are visible in outcrop and range from tight to open and gently undulating interlimb angles. It is assumed that these folds represent parasitic folding related to the larger scale horseshoe fold.

In this study, we examine the results of petrophysical, mineralogical and palaeomagnetic analyses with the aim of differentiating magnetite and hematite content in the samples and quantify the relative magnetic contribution of these and other magnetic minerals to the magnetic signature of the broader rock packages. Petrophysical measurements made as part of this study include density (i.e. specific gravity), magnetic susceptibility, anisotropy of magnetic susceptibility and remanent magnetisation. A number of methods were used to resolve the palaeomagnetic history of the samples including liquid nitrogen bathing and alternating field demagnetisation. Constrained 3D modelling of publicly available aeromagnetic data was undertaken to confirm the validity of using measurements made of surface samples as model input values.

This work was carried out as part of the Capricorn Orogen Distal Footprints research program.

METHOD AND RESULTS

Petrophysical and Magnetic Properties

A total of 74 specimens were recovered from 10 oriented block samples. Holes were drilled normal to lithological layering and the resultant cores were cut into cylinders. The specimen were prepared as standard palaeomagnetic cylinders with nominal radii and heights of 24.5 mm and 22 mm respectively. These dimensions give the closest shape approximation of a sphere.

Density and volume measurements were made on a Mettler Toledo MS204TS analytical balance using the Archimedes principle. Magnetic susceptibility and anisotropy of magnetic susceptibility (AMS) was measured using an Agico MFK1-A Kappabridge magnetometer using a field strength of 200 A/m. Thermal susceptibility measurements were also made using the Agico MFK1-A with the furnace attachment with the maximum temperature set at 700°C for each measurement run.

Remanent magnetisation was predominantly measured using a CSIRO-built fluxgate spinner magnetometer. A number of specimen were also measured using an Agico JR6A spinner magnetometer. Duplicate measurements were made on both machines to test for consistency which revealed an average difference in declination angle of less than 0.5°.

Table 1 shows the maximum, minimum and average values of the measured petrophysical properties. As would be expected of an iron formation, the petrophysical properties were quite varied. Density values range from 2.54 g/cm³ to 4.01 g/cm³ with an average of 3.47 g/cm³. Magnetic susceptibility measurements show a minimum of 6 x 10⁻⁴ SI and a maximum of 0.52 SI. The natural remanent magnetisation intensities range from 6 x 10⁻³ A/m to a staggering 1320 A/m. Magnetisation intensities this high are unusual and are discussed further below.

Table 1: Maximum, minimum and average petrophysical properties of the measured sample set.

	Density (g/cm ³)	Mag Sus (SI)	NRM (A/m)	Koenigsberger Ratio
Min	2.54	0.00062	0.0064	0.2
Avg	3.40	0.13736	203.0	28.3
Max	4.01	0.52751	1320.6	189.2

Plots of the various petrophysical measurements are shown in Figure 1 A-D. The plot of density versus magnetic susceptibility (Figure 1A) reflects the distribution of magnetite in the sample set. The large vertical spread of magnetic susceptibility values directly reflects varying levels of magnetite in the samples with those samples at the top of the plot containing significantly more magnetite than those which sit towards the bottom.

Density values in the sample suite can be divided into two major groups. The group between 2.5 – 3.0 g/cm³ (mainly HR02) are quartz dominated and contain relatively small amounts of iron oxides. The rest of the samples plot above 3.15 g/cm³ and are dominated by iron oxide minerals. HR07 shows a near-linear increase of magnetic susceptibility with density from quartz dominated samples that plot at around 2.7 g/cm³ to magnetite bearing iron oxide dominated samples that plot between 3.2 and 3.45 g/cm³. Samples that contain predominately weak to non-magnetic iron bearing minerals (e.g. goethite and hematite) plot along the bottom of the graph.

The cross plot of density and natural remanent magnetisation (NRM; J) shown in Figure 1B highlights the extremely strong remanent magnetisation of sample HR05 which has a peak magnetisation of 1320 A/m. There is a large spread of magnetisation intensities within HR05. However, even the sample with the lowest magnetisation has an intensity 70% greater than any of the other samples. The high intensities of HR05 somewhat mask the strong magnetisations of the other samples which have an average of 48 A/m and would be considered strongly magnetised in their own right.

The Koenigsberger ratio (Q) is the ratio remanent magnetisation to induced magnetisation and is useful when assessing the impact of remanent magnetisation on a rock's magnetic signature. Values increasing past 1 indicate an increasing dominance of remanent magnetisation in the sample. In the measured suite of samples, HR09 showed the highest Q value of 189 (Figure 1C). All samples averaged over 4 which indicates the ubiquitous nature of remanent magnetisation in the Horseshoe Range BIFs.

The interesting nature of the magnetic signature of HR05 is illustrated in the plot of magnetic susceptibility versus NRM in Figure 1D. Samples that contain minerals with strong remanent magnetisation relative to their susceptibility (e.g. hematite and monoclinic pyrrhotite) will plot up the left side of the graph, whereas samples with increasing magnetite content will typically plot along the bottom of the graph towards the right. The fact that HR05 plots in the upper right corner of the graph indicates the presence of single or pseudo-single domain (SD or PSD) magnetite which typically displays elevated magnetic susceptibility and strong remanent magnetisation (Clark, 1997).

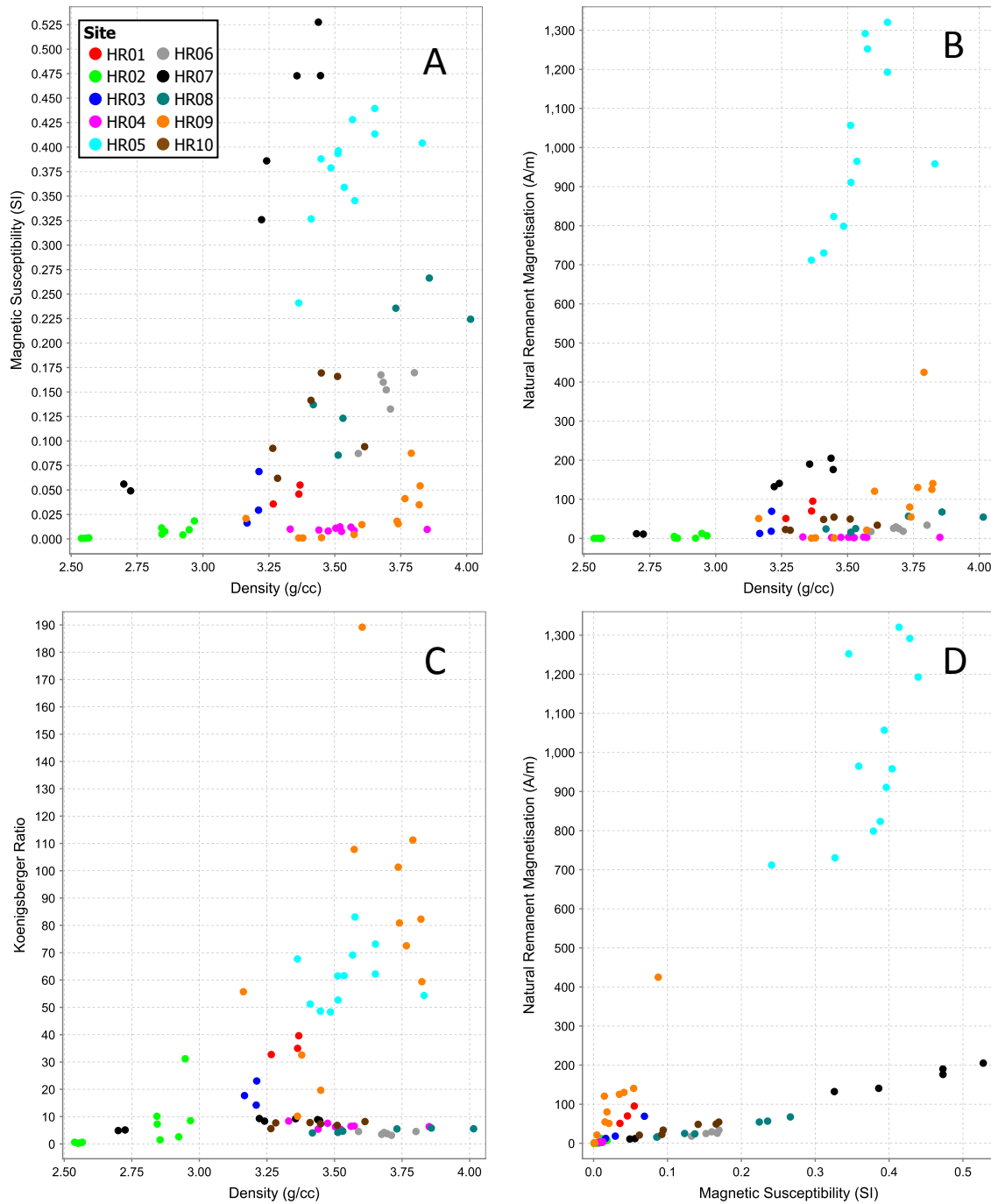


Figure 1: Cross plots of the petrophysical measurements. A) Density (g/cm^3) versus magnetic susceptibility (SI); B) Density (g/cm^3) versus natural remanent magnetisation (A/m); C) Density (g/cm^3) versus Koenigsberger ratio; D) Magnetic susceptibility (SI) versus natural remanent magnetisation (A/m).

Mineralogy

A number of methods were employed to differentiate magnetite from hematite and gain insights into the bulk mineralogy of the samples. Initially, thermal susceptibility was used to differentiate hematite from magnetite by way of observing the drop off in induced magnetisation past the Curie points of each mineral. Thermal susceptibility experiments involve crushing a sample to a powder, placing it in a precisely controlled furnace and measuring the magnetic susceptibility at increasing temperatures. All experiments were carried out with a maximum temperature of 700°C which encompassed the curie points of magnetite ($\sim 580^\circ\text{C}$) and hematite (680°C). The results of these tests indicated the presence of magnetite in all samples (Figure 2). Hematite was only clearly observable in one sample. The signal associated with magnetite often masks the response of hematite in thermal susceptibility analyses which is likely to have occurred in our testing.

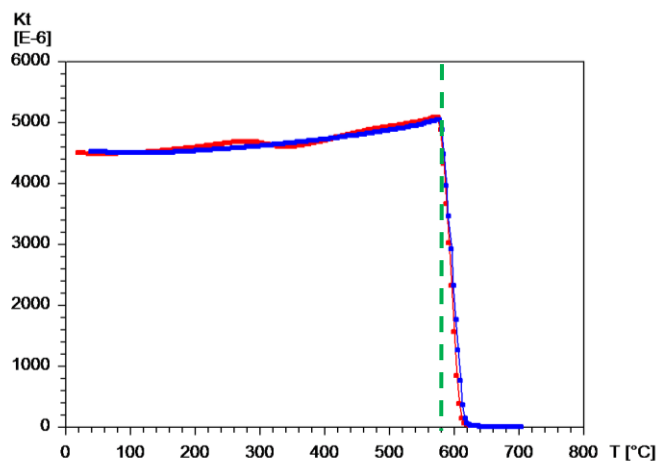


Figure 3: Plot of magnetic susceptibility versus temperature from HR07. The red line is the heating sequence and the blue is the cooling sequence. Note the Curie point at ~ 580°C which indicates the presence of magnetite.

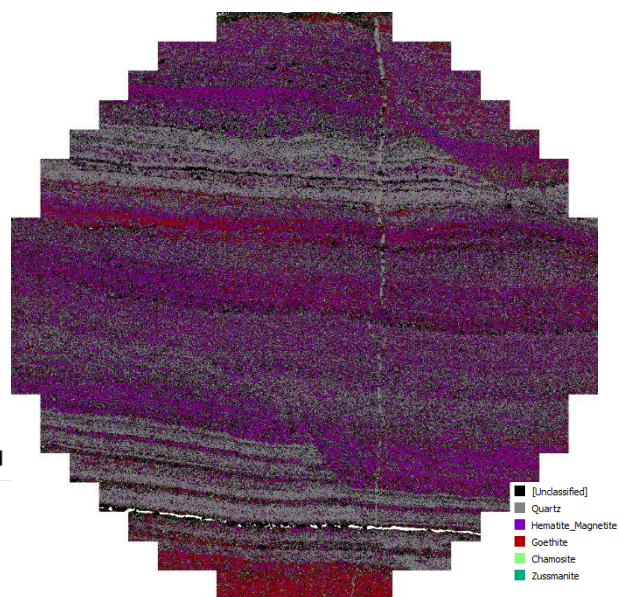


Figure 2: TIMA mineralogy map from sample HR05. Note that this method is unable to distinguish magnetite and hematite

In order to understand the strong magnetic responses of the samples, holes were drilled parallel to the lithological layers of the BIF resulting in cross sections of each bulk sample. These samples underwent scanning electron microscope (SEM), energy dispersive x-ray spectrometry (EDS) and electron back-scatter diffraction (EBSD) analyses.

Despite being relatively quick, one drawback of the TIMA (Tescan Integrated Mineral Analyser) SEM analysis is that the process cannot confidently distinguish between magnetite (Fe_3O_4) and hematite (Fe_2O_3) (Figueroa et al., 2011) as shown in Figure 3. This is obviously an issue when trying to understand the source of magnetic signals in iron formations. To solve this issue, quantitative EDS was used on a number of samples to distinguish between the two minerals. Further, electron back-scatter diffraction was used to distinguish between trigonal Fe_2O_3 (hematite) and cubic Fe_2O_3 (magnetite).

HR05 has the strongest remanent magnetisation at over 1300 A/m. EDS analysis carried out on this sample showed that single crystal magnetite is being altered to polycrystalline hematite (Figure 4). The resulting hematite is crystallographically controlled by the grain structures of the parent magnetite but does not form in a consistent lattice orientation. The extent of alteration from hematite to magnetite varies at any given point in the sample from untouched magnetite grains to fully altered polycrystalline hematite.

An important side effect of the hematite alteration is the breakdown of large multi-domain (MD) magnetite grains into smaller single or pseudo-single domain (SD or PSD) grains. MD magnetite typically displays high magnetic susceptibility and strong but unstable remanent magnetisation whereas SD or PSD magnetite often display far stronger and more stable remanent magnetisation.

The random nature of the hematite alteration results in HR05 containing a combination of MD and SD/PSD grains which can explain the elevated magnetic susceptibility and extreme remanent magnetisation discussed below.

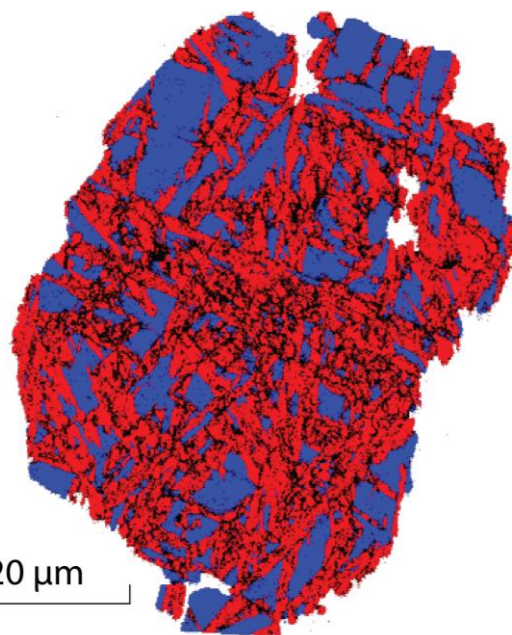


Figure 4: EBSD image from HR05 showing a euhedral magnetite grain (blue) being altered to polycrystalline hematite (red)

Remanent Magnetisation

The presence of strong remanent magnetisation can be observed in almost every sample with the exception of those sub-specimen which consist predominately of quartz. Koenigsberger ratios range from 0.3 (predominantly induced magnetisation) up to 205 (dominated by remanent magnetisation) and all but one sample have averages >5 .

Remanent magnetisation directions varied widely between the sample sites but vectors from sub-specimen from each sample were generally well clustered. One exception to this trend was HR02 which plotted both vertically up and down and coincidentally had the weakest magnetisations and lowest Q ratios. The majority of magnetisation directions plot in the lower hemisphere of the stereonet (Figure 5). In the magnetic latitude in which these samples were recovered, such magnetisations would typically create a large negative magnetic anomaly which is not seen in the aeromagnetic data.

Remanent magnetisation intensities were reduced by an average of 60% after being 'cleaned' using liquid nitrogen. This method brings the samples below the Verwey transition (Schmidt et al., 2007) and removes the softer, lower coercivity components of remanent magnetisation by slightly altering the crystalline structure of the magnetite grains. Despite the majority of samples losing significant magnetisation intensity (up to 75%), the largest change in magnetisation direction was only 16° .

Alternating Field Demagnetisation (AFD)

A selection of samples were subjected to alternating field demagnetisation (AFD) using a 2G Systems 600-Series in-line degausser with increasing field intensities from 2mT up to 140mT being applied. Magnetisation intensities dropped off quite rapidly after 10-15mT and usually reached minimum levels at around 70mT.

A number of specimens from samples HR05 and HR09 retained very stable magnetisation orientations throughout all AFD steps. Magnetisation vectors from HR05 and HR09 were oriented predominately in the same direction as their respective NRM measurements – plunging moderately to the southwest and moderately to the north respectively. HR05 displayed extremely strong remanent magnetisation (up to 1320 A/m) whereas HR09 had moderate magnetisation intensity (up to 205 A/m) but both had highly elevated Koenigsberger ratios with averages of 66 and 83 respectively. The magnetisation in HR09 appears to be dominated by hematite (i.e. less magnetite) due to the relatively low magnetic susceptibility of this sample whereas HR05 had both strong remanent magnetisation as well as high magnetic susceptibility which indicates the presence of both hematite and magnetite. The specimen from HR05 retained very stable magnetisation directions up to the peak field of 140mT. The NRM and AFD step vectors for HR05 are oriented within $15\text{-}20^\circ$ of the K1 AMS vector. Whilst this may be a coincidence, it is possible that the remanent magnetisation is being deflected away from the true palaeopole by the anisotropy of the magnetite grains (e.g., Biedermann et al., 2017)

Anisotropy of Magnetic Susceptibility (AMS)

Anisotropy of magnetic susceptibility (AMS) was measured on all specimens. AMS essentially measures grain shape elongation of magnetic minerals and results are interpreted in terms of an ellipsoid comprising of a long (K1), intermediate (K2) and short (K3) axes. The ratios between these values define the anisotropy of the specimen where the maximum anisotropy (P) is given by $K1/K3$. The average P value for the dataset is 1.12 (i.e. an anisotropy of 12%) with some samples indicating maximum anisotropy values of 1.62. Figure 6 shows the spread of results in terms of the maximum anisotropy (P v K) and the shape of the fabric (L v F) which is predominately a foliation fabric. Results from the AMS measurements are also shown in Figure 7 along with measured bedding planes from the sample sites. This data was recorded in an area with a radius of approximately 2m from the sample location. The strike measurements correspond well with the measured AMS foliation plane and the poles to these planes plot very close to the K3 short axis in all instances with the exception of HR05 (Figure 7C) where the K3 axes and poles to the bedding planes differ in strike by approximately 10° . These results are not unexpected for well layered BIFs such as those sampled in this study.

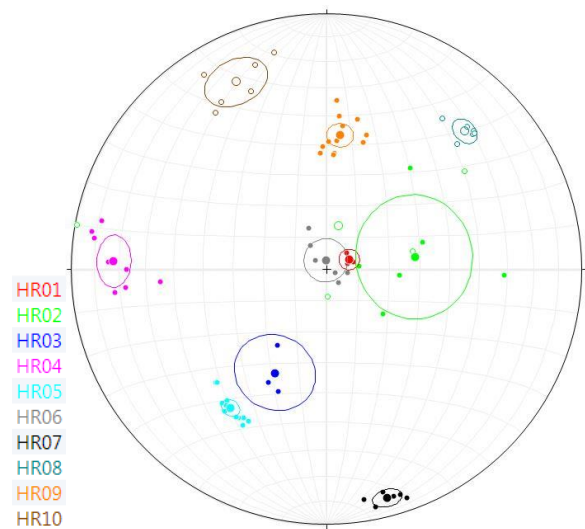


Figure 5: Stereonet projection of the measured natural remanent magnetisation vectors at Horseshoe. The colouring scheme is consistent with the petrophysical data presented above.

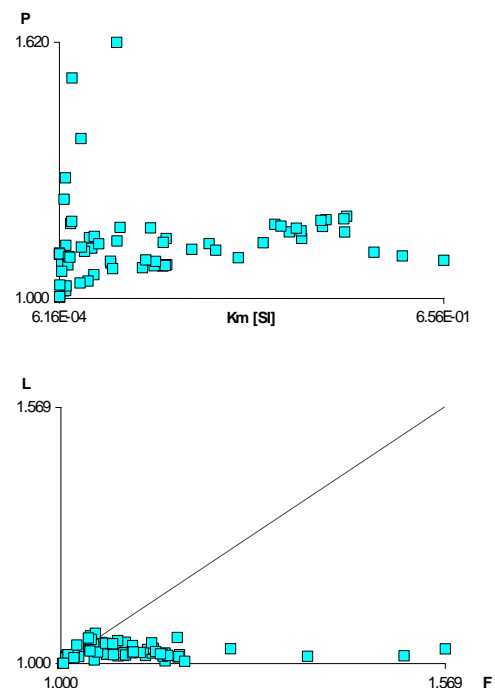


Figure 6: Plots of P ($K1/K3$) versus bulk susceptibility and Foliation ($K2/K3$) versus Lineation ($K1/K2$).

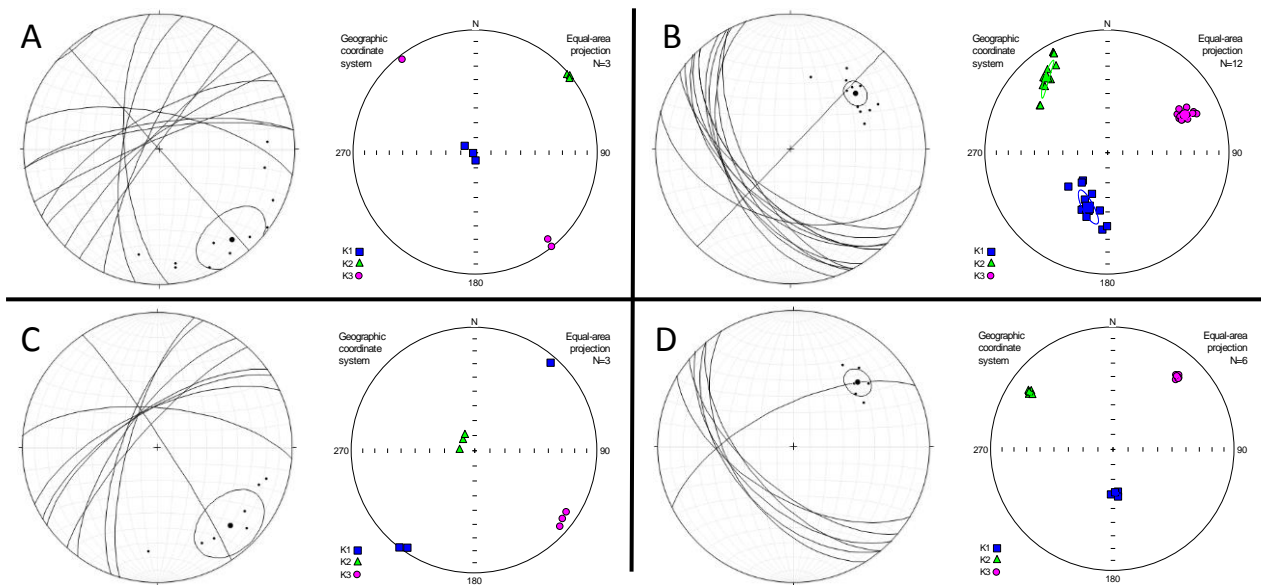


Figure 7: Measured bedding planes and the corresponding anisotropy of magnetic susceptibility (AMS) results. A) HR01, B) HR05, C) HR03, D) HR06. Blue squares = long axis (K1), green triangles = intermediate axis (K2), and pink circles = short axis (K3). Note that the foliations defined by K1 and K2 are parallel to the measured bedding planes.

3D MAGNETIC MODELLING

The modelling shown herein was based off the available aeromagnetic data available from the Geophysical Archive Data Delivery Systems (GADDS) and was modelled using ModelVisionPro™. Initially, the total magnetic intensity (TMI) data was modelled using a single homogeneous layer, albeit with a higher than measured magnetic susceptibility value. Using a single homogeneous layer to model a BIF is clearly not an accurate representation of the geology which would typically display wide variances in mineralogical and magnetic properties as shown in the petrophysical data presented above.

Using the first vertical derivative (1VD) of the TMI data as the model input allows for more accurate delineation of the magnetic structures in the Horseshoe Range BIF. The model produced to fit this data indicated four separate layers with magnetic susceptibility values that increase towards the northeast to a maximum value of 0.55 SI which is consistent with the maximum measured values (Figure 8). The bodies created in this model were oriented in accordance with structural data recorded in the field and generally dip towards the southwest.

Figure 8 shows a three profiles of the 1VD of the TMI data that have been modelled using four dipping bodies with magnetic susceptibility values constrained by petrophysical measurements made surface samples. The bodies provide an excellent fit to the data but do not have any remanent magnetisation assigned to them.

Despite resulting in an RMS error of 1%, this model did not take in to account the very strong remanent magnetisations measured in a number of the samples. The majority of the measured NRM vectors have a moderate to steep downward plunge towards the south and average Koenigsberger ratios of 30. When the proportion of remanent magnetisation in a rock package is this high, such magnetisation directions typically result in large negative anomalies as the remanent magnetisation dominates the magnetic signal. This does not appear to be the case in the TMI data over Horseshoe however. As a result, it is likely that the extreme remanent magnetisation intensities observed in the measured samples are a result of depth limited weathering and are volumetrically insignificant in terms of the broader Horseshoe formation.

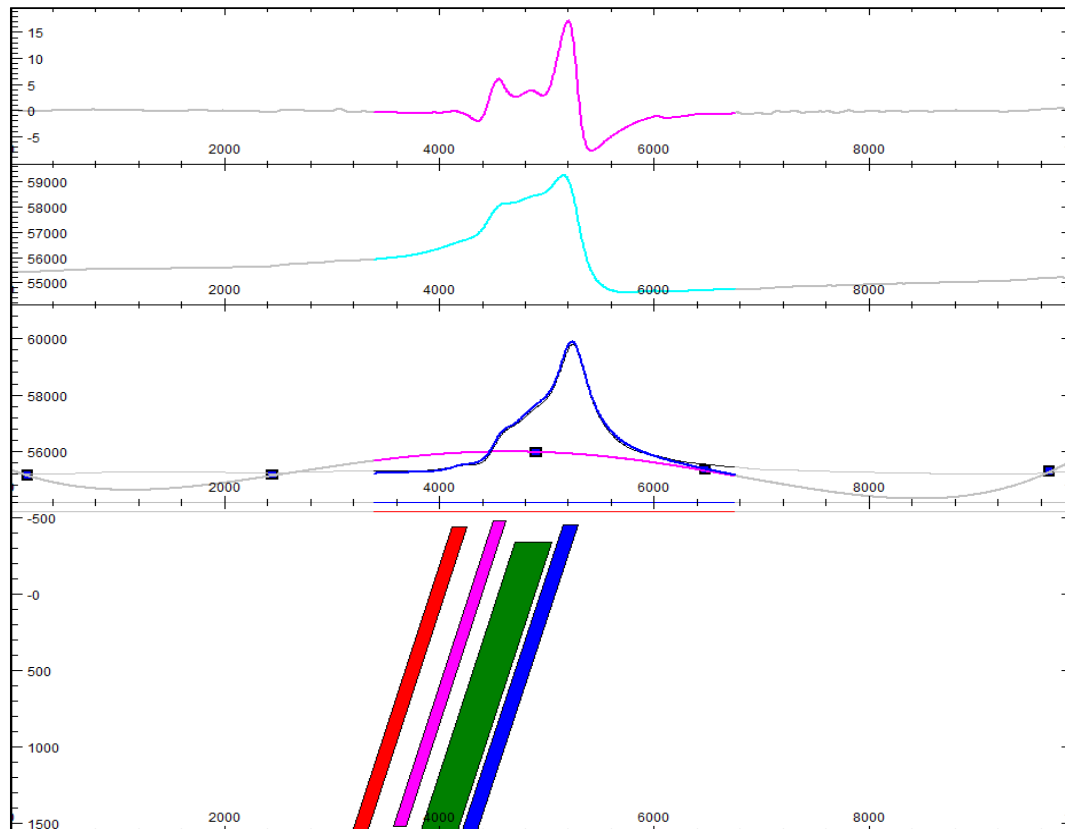


Figure 8: An example of the model created for the northern limb of the Horseshoe magnetic anomaly with three data lines active. The depth extent of the bodies has little effect on the model response below 500 m (?).

CONCLUSIONS

The Horseshoe Range iron formation presents an interesting array of magnetic signatures and petrophysical properties. As would be expected of finely layered iron formations, the basic petrophysical properties of density, magnetic susceptibility and remanent magnetisation vary widely with changes in mineralogy over millimetre to kilometre scales.

Measurements of remanent magnetisation varied from essentially zero through to extremely high values in excess of 1300 A/m. Despite wide variances of magnetisation directions between samples, the majority of the samples displayed remanent magnetisation directions oriented downwards. Clustering of NRM directions from specimen from the same bulk samples was generally good with exceptions mainly associated with samples containing large proportions of quartz. Low temperature magnetic ‘cleaning’ of selected specimen prior to alternating field demagnetisation identified the presence of multi-domain magnetite in a number of samples. During this process, up to 75% of remanent magnetisation was removed from some samples but the maximum change in magnetisation direction was only 16°. Alternating field demagnetisation results showed that some remanent magnetisation components were incredibly stable and retained the same direction throughout the entire demagnetisation process. Electron backscatter diffraction analyses revealed that the sample with the strongest remanent magnetisation (HR05) contained euhedral multi-domain magnetite grains that were being altered to polycrystalline hematite. This process results in the formation of single or pseudo-single domain magnetite grains that carry very strong and stable remanent magnetisations. The hematite alteration is seemingly random and varies in its extent at any given location in the sample. The result of this is a mix of large MD magnetite which gives the sample its high magnetic susceptibility, and small SD or PSD magnetite which create the extreme remanent magnetisation. Thermal demagnetisation is to be carried out on selected samples in order to gain more understanding of the complex remanent magnetisation that was not fully resolved using alternating field demagnetisation.

The Anisotropy of magnetic susceptibility measurements obtained are in line with what one would expect when studying a banded iron formation. The main fabric identified was a foliation defined by the long and intermediate axes that together define a fabric that is parallel with the lithological layering observed in the samples. When the results are reoriented to geographic coordinates, the measured magnetic foliation aligns well with the measured structural data.

Analysis of the aeromagnetic data does not indicate a strong negative anomaly that would typically be produced by a rock package with strong downward oriented remanent magnetisation. The TMI data can be sufficiently modelled using a very basic single layer body with an appropriate magnetic susceptibility but this approach is not geologically sensible or petrophysically valid. To better reflect the natural variation observed in banded iron formations and fully utilise the suite of petrophysical measurements, a model was

produced to fit the 1VD profiles of the aeromagnetic data. The resulting model comprised of multiple parallel bodies that fit the data very well with an RMS error of 1%. However, this model did not take into account the strong remanent magnetisation observed in the surface samples. The fact that there is no distinctive negative anomaly in the aeromagnetic data and the ability to model the data very accurately without using remanent magnetisation indicates that the hematite alteration and extreme remanence observed in this study may be limited to the very near surface or caused by natural phenomenon such as lightning strikes.

REFERENCES

Biedermann, A.R., Jackson, M., Bilardello, D., McEnroe, S.A., 2017, effect of magnetic anisotropy on the natural remanent magnetization in the MCU IVe' Layer of the Bjerkreim Sokndal Layered Intrusion, Rogaland, Southern Norway: *Journal of Geophysical Research Solid Earth*, 122, 790-807.

Clark, D.A., 1997, Magnetic petrophysics and magnetic petrology: aids to geological interpretation of magnetic surveys: *Journal of Australian Geology and geophysics*, 17(2), 83-103.

Figueroa, G., Moeller, K., Buhot, M., Gloy, G., Haberalah, D., 2011, Advanced discrimination of hematite and magnetite by automated mineralogy: *Proceedings of the 10th International Congress for Applied Mineralogy (ICAM)*, 197-204.

Schmidt, P.W., McEnroe, S.A., Clark, D.A. and Robinson, P., 2007, Magnetic properties and potential field modelling of the Peculiar Knob metamorphosed iron formation, South Australia: An analog for the source of the intense Martian magnetic anomalies?: *Journal of Geophysical Research*, 112, B03102.